Inorg. Chem. **2008**, *47*, 8091−8100

One-, Two-, and Three-Dimensional Arrays of Eu^{3+}-4,4,5,5,5-pentafluoro-1-(naphthalen-2-yl)pentane-1,3-dione complexes: Synthesis, Crystal Structure and Photophysical Properties

D. B. Ambili Raj, S. Biju, and M. L. P. Reddy*

Chemical Sciences and Technology Division, National Institute for Interdisciplinary Science & Technology (NIIST), CSIR, Thiruvananthapuram-695 019, India

Received March 15, 2008

A novel β-diketone, 4,4,5,5,5-pentafluoro-1-(naphthalen-2-yl)pentane-1,3-dione (HPFNP), which contains polyfluorinated alkyl group, as well as the long conjugated naphthyl group, has been used for the synthesis of a series of new tris(β-diketonate)europium(III) complexes of the general formula $Eu(PFNP)_3 \cdot L$ [where L = H_2O, 2,2′-bipyridine (bpy), 1,10-phenanthroline (phen), 4,7-diphenyl-1,10-phenanthroline (bath)] and characterized by various spectroscopic techniques. The single-crystal X-ray diffraction analysis of $Eu(PFNP)_3$.bpy revealed that the complex is mononuclear, the central Eu^{3+} ion is coordinated by six oxygen atoms furnished by three β-diketonate ligands, and two nitrogen atoms from a bidentate bipyridyl ligand, in an overall distorted square prismatic geometry. Further, analysis of the X-ray crystal data of the above complex also revealed interesting 1D, 2D, and 3D networks based on intra- and intermolecular hydrogen bonds. The room-temperature PL spectra of the complexes are composed of typical Eu^{3+} red emissions, assigned to transitions between the first excited state ($^5D_0$) and the multiplet ($^7F_{0-4}$). The results demonstrate that the substitution of solvent molecules by bidentate nitrogen ligands in $Eu(PFNP)_3 \cdot H_2O \cdot EtOH$ greatly enhances the quantum yields and lifetime values.

Introduction

The versatile photophysical properties of lanthanide ions have inspired vigorous research activities because of the wide range of photonic applications, such as tunable lasers, amplifiers for optical communications, luminescent probes for analytes, components of the emitting materials in multilayer organic light emitting diodes, and efficient light conversion molecular devices.[1−6] The Eu^{3+} and Tb^{3+} ions are of particular interest because of their long luminescence lifetime and narrow emission bands in the visible region.[7] Because the Laporte-forbidden 4f−4f transition prevents direct excitation of lanthanide luminescence, Ln^{3+} ions always require sensitization by suitable organic chromophores. Furthermore, for practical applications, Ln^{3+} ion must be incorporated into highly stable coordinated complexes. The efficiency of ligand-to-metal energy transfer, which requires compatibility between the energy levels of the ligand excited states and accepting levels of Ln^{3+} ions, is crucial in the design of high performance luminescent molecular devices. Moreover, ligands containing high-energy oscillators, such as C−H and O−H bonds, are able to quench the metal excited states nonradiatively, thereby leading to lower luminescence intensities and shorter excited-state lifetimes. Thus the replacement of C−H bonds with C−F bonds is important in the design of new lanthanide luminescent complexes with efficient emission properties.

The β-diketone ligand is one of the important "antennas",[8] from which the energy can be effectively transferred to Ln^{3+} ions for high harvest emissions and has the following advantages. The β-diketone ligand has strong absorption

* To whom correspondence should be addressed. E-mail: mlpreddy@yahoo.co.uk.

(1) Bünzli, J-C. G.; Piguet, C. *Chem. Soc. Rev* **2005**, *34*, 1048–1077.
(2) de Bettencourt-Dias, A. *Dalton Trans.* **2007**, 2229–2241.
(3) Kuriki, K.; Koike, Y.; Okamoto, Y. *Chem. Rev.* **2002**, *102*, 2347–2356.
(4) Kido, J.; Okamoto, Y. *Chem. Rev.* **2002**, *102*, 2357–2368.
(5) Sun, P. P.; Duan, J. P.; Lih, J. J.; Cheng, C. H. *Adv. Funct. Mater.* **2003**, *13*, 683–691.
(6) Hao, R.; Li, M.; Wang, Y.; Zhang, J.; Ma, Y.; Fu, L.; Wen, X.; Wu, Y.; Ai, X.; Zhang, S.; Wei, Y. *Adv. Funct. Mater.* **2007**, *17*, 3663–3669.
(7) (a) Yang, C.; Fu, L. -M.; Wang, Y.; Zhang, J.-P.; Wong, W.-T.; Ai, X.-C.; Qiao, Y.-F.; Zou, B.-S.; Gui, L.-L. *Angew Chem., Int. Ed.* **2004**, *43*, 5010–5013. (b) Xin, H.; Li, F. Y.; Shi, M.; Bian, Z. Q.; Huang, C. H. *J. Am. Chem. Soc.* **2003**, *125*, 7166–7167.

10.1021/ic8004757 CCC: $40.75
Published on Web 08/21/2008

within a large wavelength range for its $\pi-\pi^*$ transition and, consequently, has been targeted for its ability to sensitize the luminescence of the Ln^{3+} ions. Further it has ability to form stable and strong adducts with Ln^{3+} ions, which can have practical usage.[9,10]

Recently, a large number of highly coordinated complexes of lanthanide tris(β-diketonates) containing several nitrogen ligands such as 1,10-phenanthroline,[11,12] 2,2′-bipyridine,[13,14] 4,4′-disubstituted-2,2′-bipyridines,[15,16] and 2,2′:6′,6″-terpyridine[17,18] have been reported. Earlier reports demonstrate that the replacement of C−H bonds in a β-diketone with low-energy oscillators (C−F) is able to lower the vibrational energy of the ligand, which minimizes the energy loss caused by ligand vibration and enhances the luminescent intensity of the Ln^{3+} ion. Further because of the heavy-atom effect, which facilitates intersystem crossing, the lanthanide-centered luminescent properties are enhanced.[9,19,20] These factors have prompted us to synthesize a new β-diketone ligand, 4,4,5,5,5-pentafluoro-1-(naphthalen-2-yl)pentane-1,3-dione, which has the polyfluorinated alkyl group, as well as the long conjugated naphthyl group. The synthesized ligand has been utilized for the synthesis of various Eu^{3+} complexes with bidentate nitrogen donors and investigated their photophysical properties for possible use in OLEDs as emitting materials.

Experimental Section

Materials and Instrumentation. Commercially available chemicals [europium(III) nitrate hexahydrate, 99.9% (Arcos Organics); gadolinium(III) nitrate hexahydrate, 99.9% (Aldrich), 2-acetonaphthone 98% (Aldrich), methyl pentafluoropropionate 99% (Aldrich), sodium hydride 60% dispersion in mineral oil, (Aldrich), 2,2′-dipyridyl, 99%, (Aldrich), 4,7-diphenyl-1,10-phenanthroline, 97%, (Aldrich), 1,10-phenanthroline monohydrate (Merck)] are used without further purification. All the other chemicals used were of analytical reagent grade.

Elemental analyses were performed with a Perkin-Elmer Series 2 Elemental Analyzer 2400. A Perkin-Elmer Spectrum One FT-IR Spectrometer, using KBr (neat), was used to obtain IR spectral data, and a Bruker 300 MHz NMR spectrometer was used to obtain ^{1}H NMR spectra of the compounds in $CDCl_3$ media. Mass spectra were recorded using JEOL JMS 600 fast atom bombardment (FAB) mass spectrometer. Thermogravimetric analysis (TGA) was performed using a TGA-50 Shimadzu thermogravimetric analyzer. DSC measurements were performed on a DSC-Perkin-Elmer Pyris 6 DSC instrument at a heating rate of 10 °C/min under nitrogen atmosphere. X-ray powder diffraction (XRD) analyses were performed with a Philips X'Pert Pro diffractometer. The XRD patterns were recorded in the 5−70° 2θ range using Ni-filtered Cu Kα radiation. Optical reflectance of the powder samples and absorbance of the samples in CH_3CN solution were measured with UV−vis spectrophotometer (Shimadzu, UV-2450) with an integrated sphere attachment. Photoluminescence (PL) spectra were recorded using a Spex-Fluorolog FL3−22 spectrofluorometer with double-grating 0.22 m Spex FL3−22 monochromators and a 450W Xe lamp as the excitation source using the front face mode. The lifetime measurements were carried out at room temperature using Spex FL-1040 phosphorimeter. X-ray single-crystal data were recorded at room-temperature on a Bruker AXS (Kappa Apex II) diffractometer equipped with a CCD detector and a copper tube source. Data were processed using SAINTPLUS (SAINTPLUS, program suite for data processing, Bruker AXS, Inc., Madison, WI). Structures were solved and refined using SHELXTL.

The overall quantum yields ($\Phi_{overall}$) of the europium complexes were measured at room temperature using the technique for powdered samples described by Bril et al.,[21] through the following expression:

$$\Phi_{overall} = \left(\frac{1-r_{st}}{1-r_X}\right)\left(\frac{A_X}{A_{st}}\right)\Phi_{st} \qquad (1)$$

where, r_{st} and r_X are the diffuse reflectance (with respect to affixed wavelength) of the complexes and of the standard phosphor, respectively, and Φ_{st} is the quantum yield of the standard phosphor. The terms A_X and A_{st} represents the area under the complex and the standard emission spectra, respectively. To have absolute intensity values, $BaSO_4$ was used as a reflecting standard. The standard phosphor used was Pyrene (Aldrich), whose emission spectrum is formed as a large broadband peaking around 471 nm, with a constant Φ value (Φ_{st} = 61%, λ_{ex} = 313 nm).[22]Three measurements were carried out for each sample, so that the presented Φ value corresponds to the arithmetic mean value.

(8) (a) Lehn, J.-M. *Angew. Chem., Int. Ed. Engl.* **1990**, *29*, 1304–1319. (b) de Sa, G. F.; Malta, O. L.; de Mello Donega, C.; Simas, A. M.; Longo, R. L.; Santa-Cruz, P. A.; da Silva, E. F., Jr. *Coord. Chem. Rev.* **2000**, *196*, 165–195.

(9) (a) Sun, L.-N.; Yu, J.-B.; Zheng, G.-L.; Zhang, H.-J.; Meng, Q.-G.; Peng, C.-Y.; Fu, L.-S.; Liu, F.-Y. *Eur. J. Inorg. Chem.* **2006**, *396*, 2–3973. (b) Yu, J.; Zhou, L.; Zhang, H.; Zheng, Y.; Li, H.; Deng, R.; Peng, Z.; Li, Z. *Inorg. Chem.* **2005**, *44*, 1611–1618. (c) Fratini, A.; Richards, G.; Larder, E.; Swavey, S. *Inorg. Chem.* **2008**, *47*, 1030–1036. (d) Hasegawa, Y.; Yamamuro, M.; Wada, Y.; Kanehisa, N.; Kai, Y.; Yanagida, S. *J. Phys. Chem. A.* **2003**, *107*, 1697–1702. (e) Eliseeva, S. V.; Ryazanov, M.; Gumy, F.; Troyanov, S. I.; Lepnev, L. S.; Bünzli, J.-C. G.; Kuzmina, N. P. *Eur. J. Inorg. Chem.* **2006**, *480*, 9–4820.

(10) (a) Biju, S.; Ambili Raj, D. B.; Reddy, M. L. P.; Kariuki, B. M. *Inorg. Chem.* **2006**, *45*, 10651–10660. (b) Yang, L.; Gong, Z.; Nie, D.; Lou, B.; Bian, Z.; Guan, M.; Huang, C.; Lee, H. J.; Baik, W. P. *New J. Chem.* **2006**, *30*, 791–796. (c) Pavithran, R.; Saleesh Kumar, N. S.; Biju, S.; Reddy, M. L. P.; Alves, S., Jr.; Freire, R. O. *Inorg. Chem.* **2006**, *45*, 2184–2192. (d) Binnemans, K. *Handbook on the Physics and Chemistry of Rare Earths*, Elsevier: Amsterdam, 2005; Vol. *35*, Chapter 225, pp 107−272.

(11) (a) Christidis, P. C.; Tossidis, I. O.; Paschalidis, D. G.; Tzavellas, L. C. *Acta Crystallogr.* **1998**, *C54*, 1233–1236. (b) Watson, W. H.; Williams, R. J.; Stemple, N. R. *J. Inorg. Chem.* **1972**, *34*, 501–508.

(12) Fernandes, J. A.; Sa' Ferreira, R. A.; Pillinger, M.; Carlos, L. D.; Jepsen, J.; Hazell, A.; Ribeiro-Claro, P.; Goncalves, I. S. *J. Lumin.* **2005**, *113*, 50–63.

(13) Bekiari, V.; Lianos, P. *Adv. Mater.* **1998**, *10*, 1455–1458.

(14) Pucci, D.; Barberio, G.; Crispini, A.; Francescangeli, O.; Ghedini, M.; La Deda, M. *Eur. J. Inorg. Chem.* **2003**, *364*, 9–3661.

(15) Bellusci, A.; Barberio, G.; Crispini, A.; Ghedini, M.; La Deda, M.; Pucci, D. *Inorg. Chem.* **2005**, *44*, 1818–1825.

(16) Batista, H. J.; de Andrade, A.V. M.; Longo, R. L.; Simas, A. M.; de Sa, G. F.; Ito, N. K.; Thompson, L. C. *Inorg. Chem.* **1998**, *37*, 3542–3547.

(17) Fukuda, Y.; Nakao, A.; Hayashi, K. *J. Chem. Soc., Dalton Trans.* **2002**, 527–533.

(18) Cotton, S. A.; Noy, O. E.; Liesener, F.; Raithby, P. R. *Inorg. Chim. Acta* **2003**, *344*, 37–42.

(19) Omary, M. A.; Rawashdeh-Omary, M. A.; Diyabalanage, H. V. K.; Dias, H. V. R. *Inorg. Chem.* **2003**, *42*, 8612–8614.

(20) Grushin, V. V.; Herron, N.; LeCloux, D. D.; Marshall, W. J.; Petrov, V. A.; Wang, Y. *Chem. Commun.* **2001**, *16*, 1494–1495.

(21) Bril, A.; De Jager-Veenis, A. W. *J. Electrochem. Soc.* **1976**, *123*, 396–398.

(22) Melhuish, W. H. *J. Opt. Soc. Am.* **1964**, *54*, 183–186.

Scheme 1. Synthesis of the Ligand HPFNP

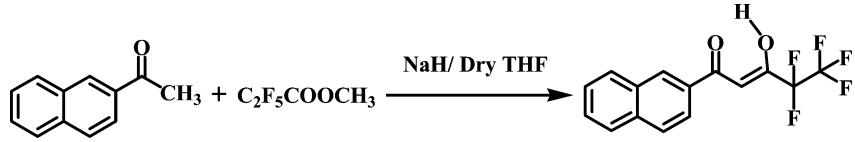

Scheme 2. Synthesis of $Ln(PFNP)_3 \cdot H_2O \cdot C_2H_5OH$

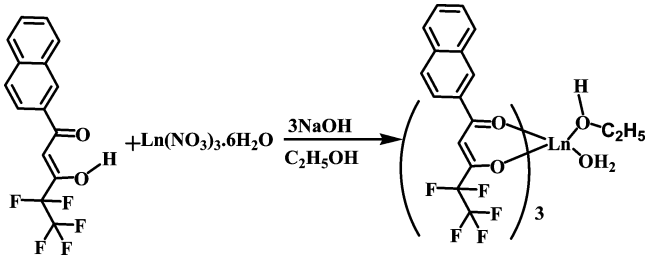

The errors in the quantum yield values associated with this technique were estimated within 10%.[23]

Synthesis of 4,4,5,5,5-Pentafluoro-1-(naphthalen-2-yl)pentane-1,3-dione (HPFNP). A modified method of typical Claisen condensation procedure is used as shown in Scheme 1. 2-Acetonaphthone (0.34 g, 0.002 mmol) and methyl pentafluoropropionate (0.356 g, 0.002 mmol) were added into 20 mL dry THF, and the mixture was stirred for 10 min. To this sodium hydride was added in inert atmosphere and stirred at room temperature for 12 h. The resulting solution was quenched with water; 2 M HCl (50 mL) was added, and the solution was extracted twice with chloroform (70 mL). The organic layer was dried over Na_2SO_4, and the solvent was evaporated to obtain a maroon oily liquid, which was purified by chromatography on a silica gel column with chloroform and hexane as the eluent to get the maroon liquid as the product (0.51 g, 80% yield). ^{1}H NMR (300 MHz, $CDCl_3$): δ 7.57−7.46 (m, 2H), δ 7.89−7.78 (m, 4H), δ 8.42 (s, 1H), δ 6.68 (s, 1H), δ 15.38 (broad, 1H). IR (KBr) ν_{max}: 3063, 1602, 1328, 1202, 1010, 795 cm^{-1}. *m*/*z* = 317 $(M + 1)^+$.

Synthesis of $Ln(PFNP)_3 \cdot C_2H_5OH \cdot H_2O$ [Ln = Eu^{3+} (1), Gd^{3+}(5)]. To an ethanolic solution of HPFNP (0.6 mmol), NaOH (0.6 mmol) is added, and the mixture was stirred for 5 min. To this a saturated ethanolic solution of $Ln(NO_3)_3 \cdot 6H_2O$ (0.2 mmol) is added dropwise and stirred for 10 h. Water is then added to this mixture, and the precipitate thus formed is filtered, washed with water, dried, and purified by recrystallization from diethyl ether−hexane mixture (Scheme 2). Unfortunately, all efforts to grow single crystals of complexes **1** and **5** were unsuccessful. Elemental analysis (%) Calcd for $C_{47}H_{32}F_{15}O_8Eu$ (**1**) (1161.70): C, 48.59; H, 2.78. Found: C, 48.92; H, 2.51. IR (KBr) ν_{max}: 3435, 1610, 1527, 1457, 1326, 1197, 1013, 792 cm^{-1}. *m*/*z* = 1120.12 ($M^+ - H_2O$, C_2H_5OH) + Na. Elemental analysis (%) Calcd for $C_{47}H_{32}F_{15}O_8Gd$ (**5**) (1166.98): C, 48.37; H, 2.76. Found: C, 48.52; H, 2.80. IR (KBr) ν_{max}: 3421, 1613, 1574, 1470, 1327, 1196, 1013, 790 cm^{-1}. *m*/*z* = 1125.05 ($M^+ - H_2O$, C_2H_5OH) + Na. Ln = Eu (**1**), Gd (**5**).

Syntheses of Complexes 2−4. Synthesis routes of the complexes **2**−**4** are shown in Scheme 3. All these complexes were prepared by stirring equimolar solutions of $Eu(PFNP)_3 \cdot C_2H_5OH \cdot H_2O$ and the nitrogen donor in $CHCl_3$ for 24 h at room-temperature. The products were obtained after solvent evaporation and are purified by recrystallization from a chloroform−hexane mixture. A crop of crystals of complex **2** were formed after ∼2 weeks. However, our efforts to grow single crystals of complexes **3** and **4** were unsuccessful.

$Eu(PFNP)_3 \cdot bpy$ (2). Elemental analysis (%) Calcd for $C_{55}H_{32}F_{15}N_2O_6Eu$ (1253.80): C, 52.69; H, 2.57; N, 2.23. Found: C, 52.77; H, 2.53; N, 2.37. IR (KBr)ν_{max}: 3058, 1637, 1610, 1594, 1507, 1473, 1328, 1281, 1197, 1162, 1013, 790 cm^{-1}. *m*/*z*= 1255.10 (M^+) + 1. mp: 200 °C.

$Eu(PFNP)_3 \cdot phen$ (3). Elemental analysis (%) Calcd for $C_{57}H32F_{15}N_2O_6Eu$ (1277.82): C, 53.58; H, 2.52; N, 2.19. Found: C, 53.62; H, 2.49; N, 2.36. IR (KBr) ν_{max}: 3056, 1609, 1592, 1568, 1506, 1327, 1279, 1197, 1153, 1009, 791 cm^{-1}. *m*/*z*= 1278.21 (M^+). mp: 185 °C.

$Eu(PFNP)_3 \cdot bath$ (4). Elemental analysis (%) Calcd for $C_{69}H_{40}F_{15}N_2O_6Eu$ (1430.03): C, 57.95; H, 2.82; N, 1.96. Found: C, 57.92; H, 2.87; N, 1.96. IR (KBr): ν_{max}: 1610, 1570, 1524, 1384, 1329, 1285, 1214, 1195, 791 cm^{-1}. *m*/*z* = 1431.12 (M^+). mp: 200 °C.

Synthesis of $Gd(bath)_2(NO_3)_3$. To a 50 mL ethanol solution containing 2.0 mmol of 4,7-diphenyl-1,10-phenanthroline, 1.0 mmol of $Gd(NO_3)_3(H_2O)_6$ was added dropwise under constant stirring, and then the solution was refluxed for 6 h at 80 °C. The resulting solution was filtered to obtain a white powder. Elemental analysis (%) Calcd for $C_{48}H_{32}N_7O_9Gd$ (1008.08): C, 57.19; H, 3.20; N, 9.72. Found: C, 57.50; H, 3.45; N, 9.72. IR (KBr) ν_{max}: 1492, 1384, 1307, 1029, 835, 766, 740, 702 cm^{-1}. *m*/*z* = 946.11 ($M^+ - NO_3$).

Results and Discussion

Structural Characterization of Europium(III) Complexes. The synthesis procedures for the europium complexes **1**−**5** are shown in Schemes 2 and 3. The microanalyses and HRMS studies of the complexes **1**−**5** shows that Ln^{3+} ion has reacted with HPFNP in a metal-to-ligand mole ratio of 1:3 and in **2**−**4,** one molecule of bidentate nitrogen ligand is involved. The IR spectrum of the complexes **1** and **5** shows a broad absorption in the region 3000−3500 cm^{-1}, indicating the presence of solvent molecules in the complex. On the other hand, the absence of the broadband in the region 3000−3500 cm^{-1} for complexes **2**−**4**, suggests that solvent molecules have been displaced by the bidentate neutral donors. The carbonyl stretching frequency of HPFNP (1602 cm^{-1}) has been shifted to longer wave numbers in complexes **1**−**5** (1610 cm^{-1} in **1**; 1613 cm^{-1} in **2**; 1610 cm^{-1} in **3**−**5**) indicating the involvement of carbonyl oxygen in the complex formation with Ln^{3+} ion. Further, the red shifts observed in the C═N stretching frequencies of nitrogen donors (1615 cm^{-1}) in complexes **2**−**4** (1594 cm^{-1} in **2**; 1592 cm^{-1} in **3**; 1598 cm^{-1} in **4**) show the involvement of nitrogen atoms in the complex formation with Eu^{3+} ion. The X-ray powder diffraction patterns of complexes **1** and **5** are similar, indicating they are isostructural and amorphous (Figure S1a). Similarly, from the XRD patterns of

(23) (a) Mello Donega, C. D.; Junior, S. A.; de Sa, G. F. *Chem. Commun.* **1996**, *11*, 1199–1200. (b) Carlos, L. D.; Mello Donega, C. D.; Albuquerque, R. Q.; Junior, S. A.; Menezes, J. F. S.; Malta, O. L. *Mol. Phys.* **2003**, *101*, 1037–1045.

Scheme 3. Synthetic Procedures for Complexes **2**−**4**

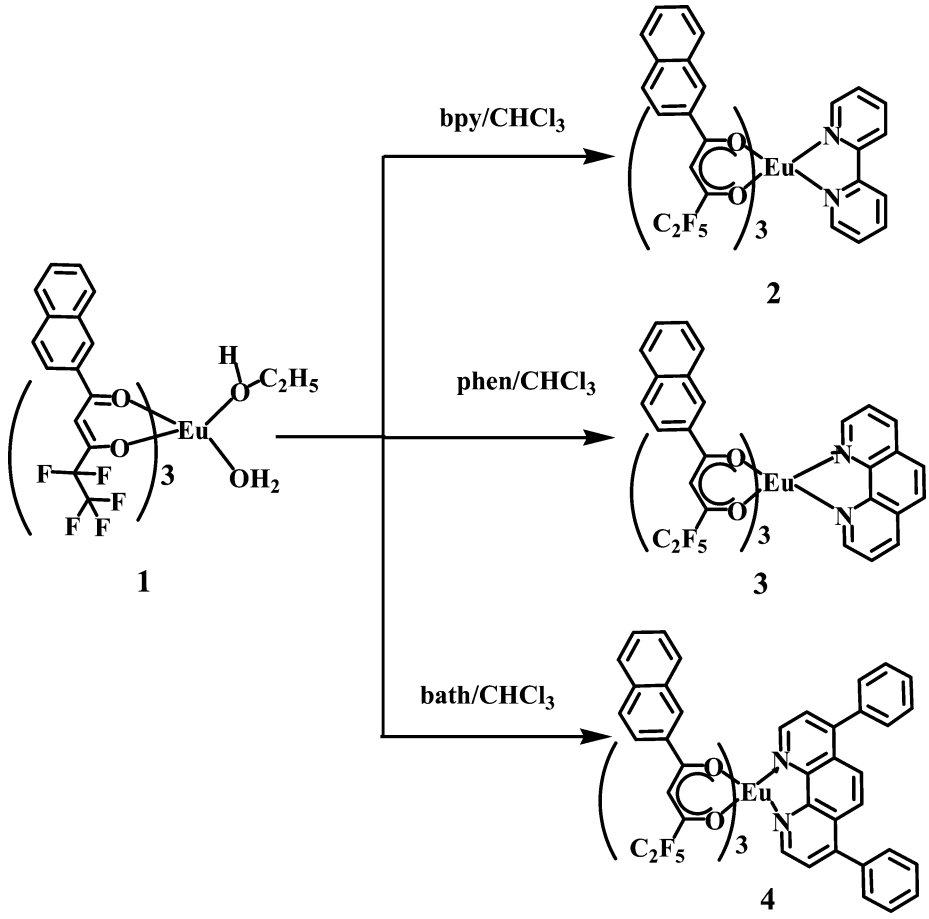

complexes **2**−**4** (Figure S1b), one can conclude that they are isostructural and crystalline.

It is clear from the thermogravimetric analysis data that complex **1** (Figure S2 in the Supporting Information) undergoes a mass loss of about 6% (calcd 5.5%) in the first step (120−230 °C), which corresponds to the elimination of the coordinated solvent molecules. Complex **1** is stable up to 230 °C, and then it under goes a single step decomposition. On the other hand, complexes **2**−**4** are more stable than the precursor sample **1**, and they undergo single-step decomposition at 275 °C. The total weight loss occurred in the TGA of all these complexes are much higher than that calculated for the thermal decomposition of these complexes into nonvolatile europium(III) oxide, indicating the partial sublimation of these complexes under atmospheric pressure, which is common in poly fluorinated β-diketonate complexes.[9e]

The DSC curve of the precursor sample (**1**) shows a shallow broad endothermic peak in the temperature range from 90−150 °C relative to the release of solvent molecules, as observed in the first event of the TG curve. Further, the absence of sharp endothermic peak in **1**, indicates the amorphous nature of the complex or at least it is difficult for it to crystallize. On the other hand, DSC curve of complexes **2**−**4** shows sharp endothermic peaks at 200, 185, and 200 °C, respectively, corresponding to their melting points (Figure S3).

X-Ray Structural Characterization. The structure of complex **2** was characterized by single-crystal X-ray crystallography. The asymmetric unit is shown in Figure 1a, and the structures with the intramolecular H-bonding interactions are shown in Figures 1b and S4. The details of crystal data and data collection parameters for complex **2** are given in Table 1. The selected bond lengths and bond angles for **2** are listed in Table 2. As predicted from the mass spectral analysis and the elemental analysis observations, the central Eu^{3+} ion is coordinated with six oxygen atoms from the three β-diketonate ligands and two nitrogen atoms from a bidentate bipyridyl ligand. The coordination geometry of the metal center is best described as a distorted square antiprism. The central Eu^{3+} ion is thus completely surrounded by the bulky aromatic anionic ligand PFNP and the synergistic bpy ligand, and this encapsulated structure therefore meets the structural requirements of an efficient lanthanide luminescent material by protecting the Eu^{3+} ion from vibrational coupling and increasing the light absorption cross-section by the so-called "antenna effect". The average Eu−N bond distance (2.56 Å) is longer than the Eu−O bonds of HPFNP ligands (2.34−2.37 Å), as observed in the X-ray single crystal data of the complexes, tris(4,4,4,-trifluoro-1-(2-naphthyl)-1,3-butanedionato)europium(III)-dipyridyl (Eu−O bonds 2.34−2.39 Å NTA; Eu−N, 2.58 Å in bpy)[24] and tris(4,4,4,-trifluoro-1-phenyl 2,4-butanedionato) europium(III)-dipyridyl (Eu−O bonds 2.32−2.40 Å in btfa; Eu−N, 2.58 Å in bpy).[16]

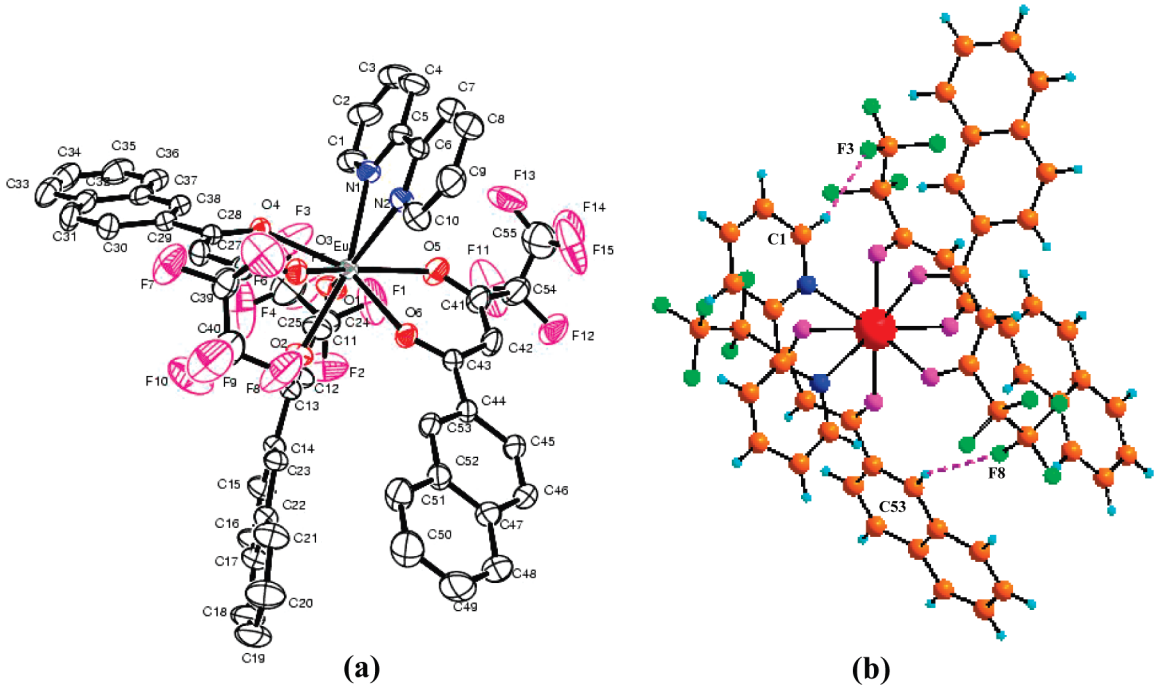

Figure 1. (a) Asymmetric unit of complex **2**. (b) Coordination environment of the Eu^{3+} ion in complex **2**. The intramolecular H-bonding interactions are shown in broken lines.

Table 1. Crystal Data, Collection, and Structure Refinement Parameters for Complex **2**

params	**2**
empirical formula	$C_{57}H_{36}Cl_3EuF_{15}N_2O_{6.50}$
fw	1396.19
cryst syst	triclinic
space group	$P\bar{1}$
cryst size (mm^3)	0.20 × 0.15 × 0.15 mm
temp (K)	293(2) K
a (Å)	10.338(4)
b (Å)	14.784(6)
c (Å)	19.431(7)
α (deg)	96.238(19)
β (deg)	93.336(18)
γ (deg)	90 96.523(19)
V ($Å^3$)	2925.7(18)
Z	2
ρ_{calcd} (g cm^{-3})	1.585
μ (mm^{-1})	1.308
F(000)	1386
R1 [$I > 2\sigma(I)$]	0.0436
wR2 [$I > 2\sigma(I)$]	0.1252
R1 (all data)	0.0520
wR2 (all data)	0.1400
GOF	1.111

Table 2. Selected Bond Lengths (Å) and Angles (deg) for Complex **2**

Eu1−N1	2.554(4)
Eu1−N2	2.570(4)
Eu1−O1	2.367(4)
Eu1−O2	2.352(3)
Eu1−O3	2.374(3)
Eu1−O4	2.336(3)
Eu1−O5	2.359(4)
Eu1−O6	2.343(3)
N1−Eu1−N2	63.03(10)
O1−Eu1−O2	71.32(18)
O3−Eu1−O4	71.92(19)
O5−Eu1−O6	71.24(18)

Further, in this complex, the Eu−O bonds adjacent to the naphthyl ring are slightly shorter than the others, which may be caused by the inductive effect of the fluorine atoms present in the HPFNP. In the *β*-diketone rings of the Eu^{3+} complex, the average distances for the C−C and C−O bonds are shorter than a single bond but longer than a double bond. This can be explained by the fact that there exists a strong conjugation between the naphthyl ring and the coordinated *β*-diketone, which leads to the delocalization of electron density of the coordinated *β*-diketonate chelate ring.[9a,25]

Two types of intramolecular interactions are observed between C1−H1···F3 and C53−H53···F8 with the distances of 2.63 and 2.83 Å, and the angles are 161.49 and 155.84°, respectively (Figure 1b). Apart from the strong intramolecular hydrogen bonding interactions, three different intermolecular hydrogen bonding interactions are also observed in **2**. Two of them form the self-assembled dimer (dimer **a** and **b**), while the third one adopts 1D structure (**c**) in the solid state. All the three interactions are shown in Figures 2 and S4. The bipyridyl ring in **A** and the napthyl ring in **D** interact with the $-CF_3$ groups of another molecule to form the self-assembled dimer and the observed interactions in C3−H3···F14 (dimer **a**) and C50−H50···F7 (dimer **b**) with the distances of 2.68 and 2.60 Å and the angles of 145.9° and 168° On the other hand, the bridging CH group and the bipyridyl group in ring **B** interact with the $-CF_3$ group of another molecule to form the rodlike 1D network. The distances and angles in 1D network are: 2.70 Å and 168° (C15−H15···F15) and 2.84 Å and 176° (C12−H12···F15). The distance between the two Eu centers is from 10.34 to 14.83 Å

(24) Thompson, L. C.; Atchison, F. W.; Young, V. G. *J. Alloys Compds.* **1998**, *275−278*, 765–768.
(25) Yu, J.; Zhang, H.; Fu, L.; Deng, R.; Zhou, L.; Li, H.; Liu, F.; Fu, H. *Inorg. Chem. Commun.* **2003**, *6*, 852–854.

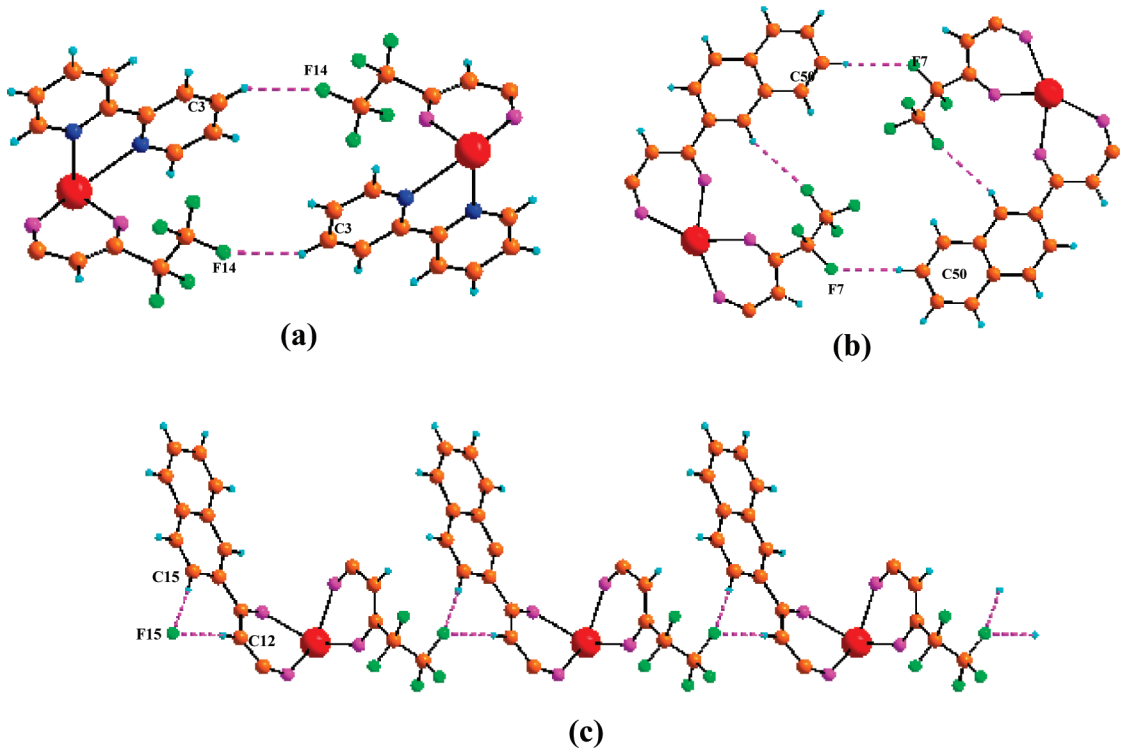

Figure 2. Self-assembled dimer and 1D network of **2**. In a, b, and c, except for the intermolecular H-bonding interactions, all the other H groups are omitted for clarity.

which is considerably longer than the Eu−Eu single bond distance.

Apart from the self-assembled dimer and 1D network, a series of 2D networks are seen in **2**. Three different 2D networks are observed: (i) the two self-assembled dimers interact with each other to form the first one. Further, each of the self-assembled dimer interacts with 1D network to form the (ii and iii) 2D networks. All the 2D networks (both the top and side views) are shown in the Supporting Information (Figure S5). Finally, all the dimers, 1D and 2D networks combine each other to form the hitherto unknown three-dimensional networks in the solid state. The observed supramolecular assembly is shown in Figure S6. To the best of our knowledge, this is the first example of Eu-β-diketonate complex which shows all the 1D, 2D, and 3D networks.

UV−vis Spectra. The UV−vis absorption spectra of the free ligand HPFNP and the corresponding Eu^{3+} complexes were measured in CH_3CN solution ($c = 1 \times 10^{-5}$ M), and are displayed in Figure 3. UV−vis absorption spectra of the neutral donors (bpy, phen, bath) are shown in Figure S8. The maximum absorption band at 345 nm for HPFNP, and the hump observed at around 333 nm in complexes **1**−**4** are attributed to singlet−singlet $\pi-\pi^*$ enol absorption of β-diketonate ligand.[26] Compared with the ligand HPFNP (λ_{max}= 345), the absorption maxima are blue-shifted to 333 nm in all the complexes. The absorption maxima at 290, 289, and 287 nm in complexes **2**−**4**, respectively, are the result of the $^1\pi-\pi^*$ absorption of the aromatic rings of bidentate nitrogen donors. These values also shows a blue shift of 7, 4, and 13 nm, respectively in complexes than in free nitrogen donors (297, 293, and 300 nm). The spectral shapes of the complexes in CH_3CN are similar to that of the free ligands, suggesting that the coordination of Eu^{3+} ion does not have a significant influence on the $^1\pi-\pi^*$ state energy. However, a small blue shift observed in the absorption maximum of all the complexes is caused by the perturbation induced by the metal coordination. The determined molar absorption coefficient values of the complexes **1**−**4** at 333 nm, 5.67×10^4, 5.7×10^4, 5.2×10^4, and 5.3×10^4 L mol^{-1} cm^{-1}, respectively, are about three times higher than that of the HPFNP (1.8×10^4 at 345 nm), indicating the presence of three β-diketonate ligands in the corresponding complexes. Further the higher molar absorp-

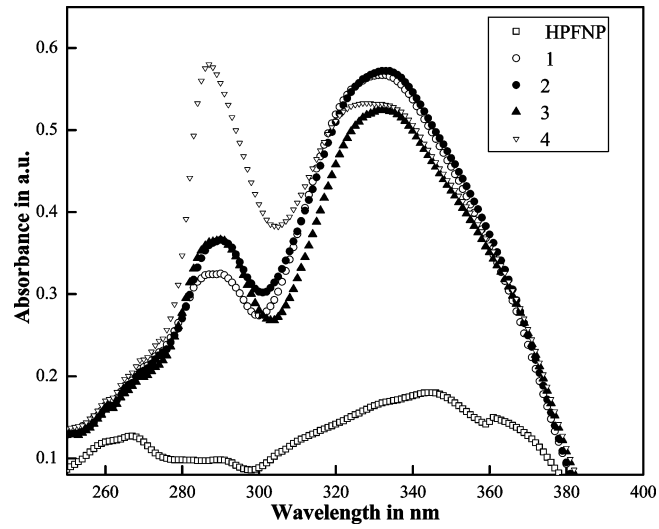

Figure 3. UV−visible absorption spectra of HPFNP and complexes **1**−**4** in acetonitrile ($c = 1 \times 10^{-5}$ M).

(26) Sun, Y.; Gao, J.; Zheng, Z.; Su, W.; Zhang, Q. *Spectrochim. Acta Part A* **2006**, *64*, 977–980.

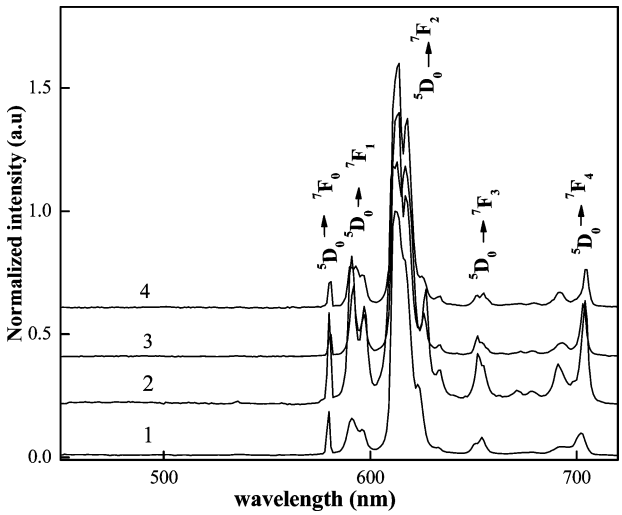

Figure 4. Room temperature (303 K) emission spectra of complexes **1**−**4**.

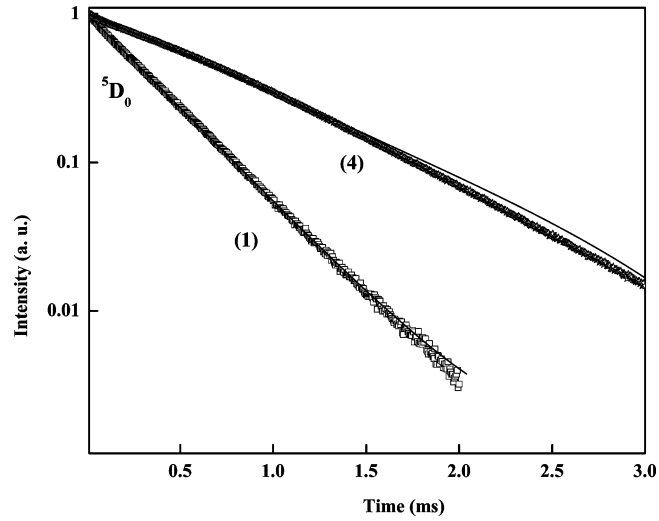

Figure 5. Experimental luminescence decay profiles of complexes **1** and **4** monitored around 612 nm and excited at their maximum emission wavelengths.

Table 3. Radiative (A_{RAD}) and Nonradiative (A_{NR}) Decay Rates, $^5D_0$ Lifetime (τ_{obs}), Intrinsic Quantum Yield (Φ_{Ln},%), Energy Transfer Efficiency ($\Phi_{transfer}$, %), and Overall Quantum Yield ($\Phi_{overall}$, %) for Complexes **1**−**4** at 303 K

complex	A_{RAD} (s^{-1})	A_{NR} (s^{-1})	τ_{obs} (μs)	Φ_{Ln} (%)	$\Phi_{transfer}$ (%)	$\Phi_{overall}$ (%)
1	899	557	687 ± 4	62	10	6
2	560	248	1238 ± 8	69	23	16
3	591	255	1183 ± 8	70	53	37
4	661	160	1218 ± 8	81	59	48

tion coefficient of HPFNP reveals that the β-diketonate ligand has a strong ability of absorbing light.

PL Properties of Complexes 1−4. The normalized excitation spectra of the Eu^{3+} complexes **1**−**4** recorded at 303 K, monitored around the intense $^5D_0 \rightarrow {}^7F_2$ transition of the Eu^{3+} ion, are shown in Figure S9. The excitation spectra of all the complexes exhibit a broadband between 250 and 450 nm and it is completely overlapped by the absorption spectra of the ligand employed in the corresponding complexes. Thus it is clear that, the central europium(III) is effectively sensitized by the coordinated ligands. A series of sharp lines assigned to transitions between the $^7F_{0,1}$ and the $^5L_6$, $^5D_{3,2,1}$ levels are also observed in the excitation spectra of all these complexes. These transitions are weaker than the absorption of the organic ligands and are overlapped by broad excitation band, which proves that luminescence sensitization via excitation of the ligand is much more efficient than the direct excitation of the europium(III) ion absorption level.

Upon excitation under the wavelengths that maximizes the europium(III) emission intensity, complexes **1**−**4** showed characteristic narrow band emissions of Eu^{3+} corresponding to the $^5D_0 \rightarrow {}^7F_J$ ($J = 0-4$) transitions (Figure 4). The five expected peaks for the $^5D_0 \rightarrow {}^7F_{0-4}$ transitions are well resolved, and the emission bands at 580 and 650 nm are very weak since their corresponding transitions $^5D_0 \rightarrow {}^7F_{0,3}$ are forbidden both in magnetic and electric dipole schemes.[27] The intensity of the emission band at 593 nm is relatively strong and independent of the coordination environment because the corresponding transition $^5D_0 \rightarrow {}^7F_1$ is a magnetic transition; on the contrary, the $^5D_0 \rightarrow {}^7F_2$ transition is an induced electric dipole transition and its corresponding intense emission at $\lambda = 613$ nm is very sensitive to the coordination environment.[27] This very intense $^5D_0 \rightarrow {}^7F_2$ peak, pointing to a highly polarizable chemical environment around the Eu^{3+} ion and is responsible for the brilliant red emission of these complexes. A relevant feature may be noted for the complexes **1**−**4** is the very high intensity of $^5D_0 \rightarrow {}^7F_2$ transition, relative to the$^5D_0 \rightarrow {}^7F_1$ lines, indicating that the Eu^{3+} ion coordinated in a local site without an inversion center. Further, the emission spectra of the complexes show only one peak for $^5D_0 \rightarrow {}^7F_0$ transition and three stark components for $^5D_0 \rightarrow {}^7F_1$ transition indicating the presence of a single chemical environment around the Eu^{3+} ion.

The $^5D_0$ lifetime values (τ_{obs}) were determined from the luminescent decay profiles for the complexes **1**−**4** at room-temperature by fitting with a monoexponential curve, indicating the presence of single chemical environment around the emitting Eu^{3+} ion and the values are depicted in Table 3. Typical decay profiles of complexes **1** and **4** are shown in Figure 5. The relatively shorter lifetime observed for complex **1** may be caused by dominant nonradiative decay channels associated with vibronic coupling because of the presence of solvent molecules, as well documented in many of the hydrated europium β-diketonate complexes.[9,10] On the other hand, longer lifetime values have been observed for complexes **2**−**4** because of the absence of nonradiative decay pathways (Figure S10 in Supporting Information).

The overall quantum yield ($\Phi_{overall}$) for a lanthanide complex treats the system as a "black box", in which the internal process is not explicitly considered. Given that the complex absorbs a photon (i.e., the antenna is excited), the overall quantum yield can be defined as[28]

$$\Phi_{overall} = \Phi_{transfer}\Phi_{Ln} \quad (2)$$

Here $\Phi_{transfer}$ is the efficiency of energy transfer from the ligand to Eu^{3+}, and Φ_{Ln}represents the intrinsic quantum yield of the lanthanide ion, which can be calculated as

$$\Phi_{Ln} = A_{RAD}/(A_{RAD} + A_{NR}) = \tau_{obs}/\tau_{rad} \quad (3)$$

The radiative lifetime (τ_{rad}) can be calculated using eq 4,[29] assuming that the energy of the $^5D_0 \rightarrow {}^7F_1$ transition (MD) and its oscillator strength are constant

$$A_{RAD} = 1/\tau_{rad} = A_{MD,0} n^3 (I_{tot}/I_{MD}) \quad (4)$$

where, $A_{MD,0}(14.65\ s^{-1})$ is the spontaneous emission probability of the $^5D_0 \rightarrow {}^7F_1$ transition in vacuo, I_{tot}/I_{MD} is the ratio of the total area of the corrected Eu^{3+} emission spectrum to the area of the $^5D_0 \rightarrow {}^7F_1$ band, and n is the refractive index of the medium. An average index of refraction equal to 1.5 was considered.[10a]

Table 3 gives the radiative (A_{RAD}) and nonradiative (A_{NR}) decay rates, $^5D_0$ lifetime (τ_{obs}), intrinsic quantum yield (Φ_{Ln}), energy transfer efficiency ($\Phi_{transfer}$), and overall quantum yield ($\Phi_{overall}$) for complexes **1**−**4** at 303 K. According to energy gap theory, radiation less transitions is prompted by ligands and solvents with high frequency vibrational modes. Creation of Eu^{3+} complexes with higher quantum yields is directly linked to suppression of radiation less transitions caused by vibrational excitations in surrounding media.[30,31] It is clear from the Table 3 that complex **1,** having solvent molecules in the coordination sphere exhibits lower overall quantum yield and lifetime values. This is caused by the presence of O−H oscillators in this system, which effectively quenches the luminescence of the Eu^{3+} ion. On the other hand, complexes **2**−**4** exhibit high overall quantum yield and lifetime values because of the displacement of solvent molecules from the coordination sphere by the bidentate nitrogen donors. Among complexes **2**−**4**, **3** and **4** exhibits better quantum yields than **2** because of the presence of additional aromatic chromophore moieties in the bidentate nitrogen donors. Considerable enhancement in the luminescent intensity noticed, especially in complex **4** can be explained on the basis of extended conjugation induced by the introduction of two phenyl groups in the 4, 7- positions of the phenanthroline ligand. It is notable from the present investigations that the intrinsic quantum yield and $^5D_0$ lifetime values obtained for Eu^{3+} complexes **2**−**4** are significantly higher than that of Eu^{3+}-naphthoyltrifluoroacetone-phenanthroline ($\Phi_{Ln} = 40\%$; $\tau_{obs} = 662\ \mu s$).[12] or Eu^{3+}-naphthoyltrifluoroacetone-bipyridyl complexes ($\Phi_{Ln} = 51\%$; $\tau_{obs} = 620\ \mu s$).[31]

Energy Transfer Processes between Ligands and Eu^{3+}. In general, the sensitization pathway in luminescent Eu^{3+} complexes consists of excitation of the ligands into their excited singlet states, subsequent intersystem crossing of the ligands to their triplet states, and the energy transfer from the triplet state to the ^5D_J manifold of the Eu^{3+} ions, followed by internal conversion to the emitting $^5D_0$ state. Finally, the Eu^{3+} ion emits when transition to the ground-state occurs.[32] Moreover, the electron transition from the higher excited states, such as $^5D_3$ (24 800 cm^{-1}), $^5D_2$ (21 200 cm−1), and $^5D_1$ (19 000 cm^{-1}) to $^5D_0$ (17 500 cm^{-1}) becomes feasible by internal conversion, and most of the photophysical processes take place in this orbital. Consequently, most Eu^{3+} complexes give rise to typical emission bands at ~581, 593, 614, 654, and 702 nm corresponding to the deactivation of the excited state $^5D_0$ to the ground states ^7F_J ($J = 0-4$). Thus, matching the energy levels of the triplet state of the ligands to $^5D_0$ of Eu^{3+} is one of the key factors that affect the luminescent properties of the europium complexes.

It is well-known that in organolanthanide complexes neutral ligands often play a role in absorbing and transporting energy to other ligands or to the central metal ion.[33] For energy transfer to occur efficiently, the overlap between the emission spectrum of the donor and the absorption spectrum of the acceptor is essential.[34] Considering complex **2** as a typical example, the possible energy transfer channels are explained from the absorption and emission spectra of the ligands. According to absorption and photoluminescence spectra of HPFNP and bidentate nitrogen donors (Figures S11−S13 for bpy, phen and bath), it is clear that there is an overlap between the room-temperature emission spectrum of bidentate nitrogen donors and the absorption spectrum of the HPFNP (from 315−395 nm for bpy; 340−395 nm for phen; 350−395 nm for bath). It means that the radiations from the singlet state of bidentate nitrogen donor can be absorbed by the β-diketonate ligand. The singlet state of nitrogen donor can also transfer energy to the triplet level of HPFNP or to its own triplet level (overlap between the room-temperature emission of bpy with the low-temperature emission spectra of HPFNP). The singlet level of HPFNP can transfer energy to the emitting level of metal ion through its own triplet energy level (overlap between the room-temperature and low-temperature emission of HPFNP). The triplet level of neutral ligand, bpy can also transfer energy to the central Eu^{3+} ion directly or through the triplet state of HPFNP (low-temperature emission spectra of bpy and HPFNP are overlapped). Thus the energy transfer process can be summarized in four steps (Figures 6 and S14). Absorbed energy is transferred from the singlet state of bpy to that of the singlet state of HPFNP, then from singlet excited-state to triplet state of the HPFNP or from singlet

(27) Werts, M. H. V.; Jukes, R. T. F.; Verhoeven, J. W. *Phys. Chem. Chem. Phys.* **2002**, *4*, 1542–1548.
(28) (a) Xiao, M.; Selvin, P. R. *J. Am. Chem. Soc.* **2001**, *123*, 7067–7073. (b) Quici, S.; Cavazzini, M.; Marzanni, G.; Accorsi, G.; Armaroli, N.; Ventura, B.; Barigelletti, F. *Inorg. Chem.* **2005**, *44*, 529–537. (c) Comby, S.; Imbert, D.; Anne-Sophie, C.; Bünzli, J.-C. G.; Charbonniere, L. J.; Ziessel, R. F. *Inorg. Chem.* **2004**, *43*, 7369–7379.
(29) (a) Viswanathan, S.; de Bettenacourt-Dias, A. *Inorg. Chem.* **2006**, *45*, 10138–10146. (b) Kim, Y. H.; Baek, N. S.; Kim, H. K. *Chem. Phys. Chem.* **2006**, *7*, 213–221.
(30) (a) Peng, C.; Zhang, H.; Yu, J.; Meng, Q.; Fu, L.; Li, H.; Sun, L.; Guo, X. *J. Phys. Chem. B.* **2005**, *109*, 15278–15287. (b) Wada, Y.; Okubo, T.; Ryo, M.; Nakazawa, T.; Hasegawa, Y.; Yanagida, S. *J. Am. Chem. Soc.* **2000**, *122*, 8583–8584.
(31) Fu, L.; Sa' Ferreira, R. A.; Silva, N. J. O.; Fernandes, J. A.; Ribeiro-Claro, P.; Goncüalves, I. S.; de Zea Bermudez, V.; Carlos, L. D. *J. Mater. Chem.* **2005**, *15*, 3117–3125.
(32) (a) Bünzli, J.-C. G. In *Lanthanide Probes in Life, Chemical and Earth Sciences*; Bünzli, J.-C. G., Choppin, G. R., Eds.; Elsevier: Amsterdam, 1989. (b) Huang, C. H.; Ed. *Coordination Chemistry of Rare Earth Complexes*; Science Press: Beijing, 1997.
(33) Xu, H.; Wang, L.-H.; Zhu, X.-H.; Yin, K.; Zhong, G.-Y.; Hou, X.-Y.; Huang, W. *J. Phys. Chem. B.* **2006**, *110*, 3023–3029.
(34) (a) Forster, T. *Z. Naturforsch.* **1949**, *A4*, 321. (b) Berlman, I. B. *Energy Transfer Parameters of Aromatic Compunds*; Academic Press: New York, 1973.

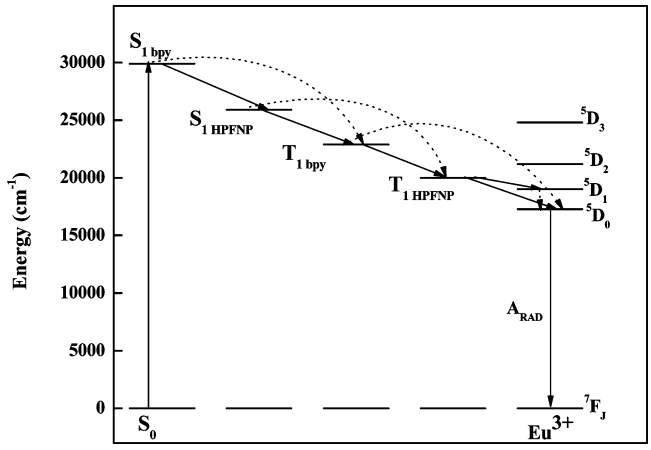

Figure 6. Schematic energy level diagram and energy transfer processes for complex **2**. S_1 represents the first excited singlet state, and T_1 represents the first excited triplet state.

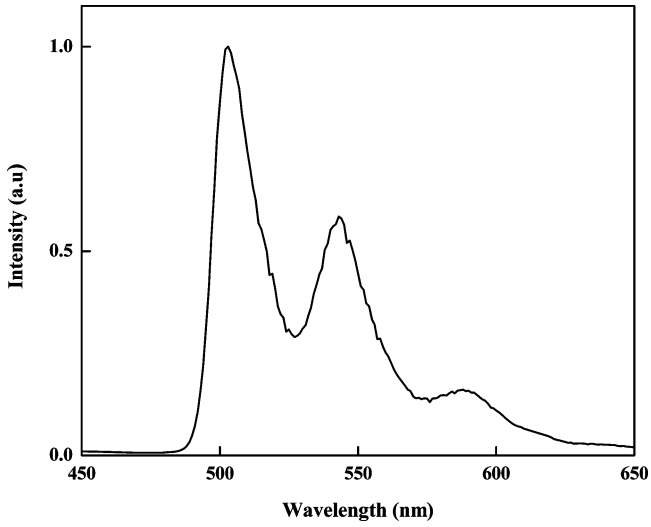

Figure 7. Phosphorescence spectra of $Gd(PFNP)_3 \cdot H_2O \cdot C_2H_5OH$ at 77 K.

excited-state of HPFNP to the triplet state of bpy. The triplet state of bpy can transfer energy to the emitting level of Eu^{3+} ion directly or through the triplet level of HPFNP. Finally, energy transfers from triplet excited-state of HPFNP to the emitting level of Eu^{3+}.

To elucidate the energy transfer process of the Eu^{3+} complexes, the energy levels of the relevant electronic states of the ligands have been determined. The singlet and triplet energy levels of HPFNP and bidentate nitrogen donors were estimated by referring to their wavelengths of UV−vis absorbance edges and the lower wavelength emission edges of the corresponding phosphorescence spectra. The triplet energy level of the ligand was not affected significantly by the Ln^{3+} ion, and the lowest-lying excited level ($^6P_{7/2} \rightarrow {}^8S_{7/2}$) of Gd^{3+} is located at 32 150 cm^{-1}.[35] On this basis, the phosphorescence spectra of $Gd(PFNP)_3 \cdot C_2H_5OH \cdot H_2O$ (Figure 7) and $Gd(bath)_2(NO_3)_3$ (Figure S15) allow one to evaluate the triplet energy levels ($^3\pi\pi^*$) corresponding ligand anions for all the lanthanide chelates. From the phosphorescence spectra, the triplet energy levels of $Gd(PFNP)_3 \cdot C_2H_5OH \cdot H_2O$ and $Gd(bath)_2(NO_3)$, which correspond to their lower emission edge wavelengths, are 20 000 (500 nm) and 21 000 cm^{-1} (476 nm), respectively. The singlet energy levels ($^1\pi\pi^*$) of HPFNP and 4,7-diphenyl-1,10-phenanthroline are estimated by referencing their higher absorption edges, which are 25 900 (386 nm) and 29 000 cm^{-1} (344 nm), respectively. The singlet and triplet energy levels of bpy (29 900 and 22 900 cm^{-1}) and phen (31 000 and 22 100 cm^{-1}) were taken from the literature.[36]

According to Reinhoudt's empirical rule,[37] the intersystem crossing process becomes effective when $\Delta E(^1\pi\pi^* - {}^3\pi\pi^*)$ is at least 5000 cm^{-1}. The energy gap $\Delta E(^1\pi\pi^* - {}^3\pi\pi^*)$ for HPFNP, bpy, phen, bath are 5900, 7000, 8900, and 8000 cm^{-1}, respectively. Thus, the intersystem crossing is effective in all the ligands. According to the empirical rule proposed by Latva, for an optimal ligand-to-metal energy transfer process $2500 < \Delta E(^3\pi\pi^* - {}^5D_0) > 3500$ cm^{-1} for Eu^{3+}.[38] It is also noted that the energy gaps, $\Delta E(^3\pi\pi^* - {}^5D_0)$ of the HPFNP, bpy, phen, and bath are 2500, 5400, 4600, and 3500 cm^{-1}, respectively. The triplet energy levels of HPFNP (20 000 cm^{-1}), bpy (22 900 cm^{-1}), phen (22 100 cm^{-1}), and bath (21 000 cm^{-1}) are higher than the $^5D_0$ level of Eu^{3+} (17 500 cm^{-1}), and also their energy gaps are too high to allow an effective back energy transfer. The schematic energy level diagrams for the complexes **1**−**4** are shown in Figures 6 and S14. Luminescence studies demonstrated that the 4,4,5,5,5-pentafluoro-1-(naphthalen-2-yl)pentane-1,3-dione ligand exhibits a good antennae effect with respect to the Eu^{3+} ion because of efficient intersystem crossing and ligand-to-metal energy transfer. Moreover, the triplet state of the 4,4,5,5,5-pentafluoro-1-(naphthalen-2-yl)pentane-1,3-dione ligand is located at 20 000 cm^{-1}, which results in a sizable sensitization of the Eu^{3+}-centered luminescence.

Conclusions

Based on the novel β-diketone, HPFNP, four new Eu^{3+} complexes **1**−**4** have been synthesized, one of which has been structurally characterized by single crystal X-ray crystallography. The X-ray crystal structure of $Eu(PFNP)_3$.bpy reveals a distorted square antiprismatic around the Eu^{3+} atom. Further, analysis of the X-ray crystal data reveals interesting one-, two-, and three-dimensional arrays of Eu^{3+}-4,4,5,5,5-pentafluoro-1-(naphthalen-2-yl)pentane-1,3-dione-2,2′-bipyridine complex through intra- and intermolecular hydrogen bonds. The luminescent studies demonstrates that the displacement of solvent molecules by bidentate nitrogen donors in $Eu(PFNP)_3 \cdot C_2H_5OH \cdot H_2O$ greatly enhances the metal-centered luminescence quantum yields and lifetime values. The introduction of polyfluorinated alkyl group, as well as long conjugated naphthyl group in β-diketonate ligand, significantly improves the intrinsic luminescent quantum yields of Eu^{3+} ion in complexes **1**−**4**

(35) Dieke, G. H. *Spectra and Energy Levels of Rare Earth Ions in Crystals*; Wiley-Interscience: New York, 1968.

(36) Yu, X.; Su, Q. *J. Photochem. Photobiolog. A: Chem.* **2003**, *155*, 73–78.

(37) Steemers, F. J.; Verboom, W.; Reinhoudt, D. N.; van der Tol, E. B.; Verhoeven, J. W. *J. Am. Chem. Soc.* **1995**, *117*, 9408–9414.

(38) Latva, M.; Takalo, H.; Mukkala, V. -M.; Matachescu, C.; Rodriguez-Ubis, J. C.; Kankare, J. *J. Lumin.* **1997**, *75*, 149–169.

(62−81%) as compared to existing Eu^{3+}-naphthoyltrifluoroacetone-nitrogen donor complexes (40−50%). Thus our results clearly highlights that Eu^{3+}-4,4,5,5,5-pentafluoro-1-(naphthalen-2-yl)pentane-1,3-dione complexes involving bidentate nitrogen donors may find potential applications as light conversion molecular devices in many photonic applications.

Acknowledgment. The authors acknowledge financial support from the Council of Scientific and Industrial Research (NWP0023), Defence Research and Development Organization, and University Grants Commission, New Delhi. The authors also thank Prof. T. K. Chandrashekar, Director, and Dr. Suresh Das, Head, Chemical Sciences & Technology Division, and Dr. A. Srinivasan, National Institute for Interdisciplinary Science & Technology (NIIST), Trivandrum, India, for their constant encouragement and valuable discussions. Dr. Babu Varghese, Senior Scientific Officer Grade I, SAIF, IIT-Madras, is also acknowledged for X-Ray crystallographic analysis.

Supporting Information Available: Crystallographic data, TG data, luminescence decay profiles, phosphorescence spectrum, absorption and emission spectra of HPFNP, bpy, and phen at 303 and 77 K in CH_3CN solution, and schematic energy level diagram. This material is available free of charge via the Internet at http://pubs.acs.org.

IC8004757